International Immunopharmacology 75 (2019) 105770

Contents lists available at ScienceDirect

International Immunopharmacology

journal homepage: www.elsevier.com/locate/intimp

Glutaminyl cyclase inhibitor exhibits anti-inflammatory effects in both AD and LPS-induced inflammatory model mice

Xiaojuan Wang[a,1], Li Wang[b,1], Xi Yu[a], Yue Li[a], Zhigang Liu[c], Yongdong Zou[b], Yizhi Zheng[b], Zhendan He[a], Haiqiang Wu[a,b,*]

[a] School of Pharmaceutical Sciences, Health Science Center, Shenzhen University, Shenzhen 518055, China
[b] College of Life Sciences and Oceanography, Shenzhen University, Shenzhen 518055, China
[c] School of Basic Medical Science, Health Science Center, Shenzhen University, Shenzhen 518055, China

ARTICLE INFO

Keywords:
Glutaminyl cyclase
Alzheimer's disease
Inflammation
Inhibitor
Anti-inflammatory effect

ABSTRACT

Up-regulated glutaminyl cyclase (QC) plays crucial roles in the initiation of Alzheimer's disease (AD) and kinds of chronic diseases mediated by inflammation. QC is supposed as a novel target for the therapeutics of these diseases. Here, we explored the anti-inflammation effects of diphenyl conjugated imidazole (DPCI) derivatives which were previously designed, synthesized and evaluated as novel QC inhibitors for AD treatment in our lab. Behavioral tests, QC activity assay, histology and ELISA analysis were conducted on both AD and lipopolysaccharides (LPS)-induced inflammatory model mice. It was shown that behavioral and cognitive performance in AD mice treated with the selected compound **DPCI-23** were enhanced notably. QC activity, the formation of pE-Aβ and Aβ plaques and the activation of astrocytes and microglia cells in AD mice brains were inhibited, and the levels of inflammatory factors such as IL-6, IL-1β and TNF-α in serum were reduced remarkably. Furthermore, elevated QC activity in inflammatory mice brains was also inhibited, and levels of IL-1β, IL-1ra, TNF-α and CCL2 in serum, kidneys and brains together with the activated astrocytes and microglia cells in brains were all repressed significantly after the treatment of **DPCI-23**. These findings observed in this research demonstrated the anti-inflammation potency of **DPCI-23** in modal of AD and inflammation by inhibiting QC activity, and may contribute to the employment of QC inhibitors for the prevention and treatment of AD and other inflammatory diseases.

1. Introduction

Pyroglutamate (pE) residue, post-translationally formed from a glutaminyl precursor, constitutes the N-terminus of kinds of peptides, proteins and hormones [1]. This modification is commonly required for the maturation of proteins, enhanced lipophilicity, increased proteolytic resistance, intensified recognition and interaction with receptors [1,2]. Investigations *in vitro* and *in vivo* indicate that the formation of pE is mainly catalyzed by glutaminyl cyclase (E.C. 2.3.2.5, QC, also known as QPCT), an enzyme secreted from secretory granules in expressing cells and distributed mainly in the brain and liver of mammals, or by isoQC (also known as QPCTL) which is exclusively localized within the Golgi complex in different organs [3,4].

However, abnormal up-regulation of QC/isoQC is supposed as the key factor engaging in the initiation and development of many chronic diseases. Alzheimer's disease (AD), the most common form of dementia, is a progressive neurodegenerative disorder characterized by evident memory loss, cognitive impairments and functional decline, which inevitably leads to incapacitation and death [5]. So far, effective and safe pharmacologic agents can be offered to prevent or cure AD in clinical are insufficient. Although a great deal of efforts has been made in the past decades, the pathogenesis of AD is still unclear. Recently, a variety of N-truncated β-amyloid (Aβ) peptides have been identified in AD brains, especially pE-Aβs, which are the main components of senile plaques (> 50% of total plaques) [6–8]. Compared with normal Aβs, pE-Aβs exhibit higher proteolytic resistance and much stronger neurotoxicity [8–11]. pE-Aβs promote the formation of plaques by seeding further Aβ aggregation due to its increased hydrophobicity and can be detected much earlier than other bio-markers [11,12]. It has been confirmed that the generation of pE-Aβs is mainly catalyzed by QC in AD brains, and the reducing of pE-Aβs by inhibiting the activity of QC is helpful for the prevention and treatment of AD in different models

* Corresponding author at: School of Pharmaceutical Sciences, Health Science Center, Shenzhen University, Shenzhen 518055, China.
E-mail address: wuhq@szu.edu.cn (H. Wu).
[1] These authors contributed equally to this work.

https://doi.org/10.1016/j.intimp.2019.105770
Received 19 March 2019; Received in revised form 13 July 2019; Accepted 18 July 2019
Available online 01 August 2019

[13–20].

Meanwhile, up-regulated QC boosts acute and chronic inflammatory reactions *in vivo* [1]. In brains of AD individuals and animals, activated microglia cells and astrocytes distribute around Aβ plaques and induce neuro-inflammation by secreting a large amount of inflammatory components [21,22]. And these secreted inflammatory molecules will activate more microglia and astrocytes to generate more inflammatory mediators in turn. It has been demonstrated that QC plays a dominant role in the inflammation at early stages of AD by catalyzing the generation of pE-Aβs and pE modified inflammatory molecules such as monocyte chemoattractant protein-1 (MCP-1, also designated CCL2) which is associated with a faster rate of cognitive decline [1,23]. Furthermore, inflammation correlates with tumor progress in kinds of cancers although the mechanism in details needs further investigation. For instance, significant up-regulation of QC (not iso-QC) was identified in the pathological tissues of human thyroid carcinomas [24]. Septic arthritis caused mainly by *Staphylococcus aureus* is a severe and rapidly debilitating disease. QC inhibitors exerted strong anti-inflammatory potency in an animal model of *S. aureus*-induced septic arthritis by reducing the levels of synovitis, bone erosion, myeloperoxidase in synovial tissue, affecting the expression pattern of adhesion molecules, and preventing the up-regulation of cells expressing CD11b/CD18 [25]. In a mouse model of non-alcoholic fatty liver disease, inflammatory responses were inhibited significantly after the treatment of QC inhibitor through lowing collagen deposition and the number of F4/80-positive macrophages in liver parenchyma [26]. This research indicated that QC inhibitors may present a promising class of anti-non-alcoholic steatohepatitis agents due to their disease-modifying effects. Besides, up-regulated QC is involved in the pathology of Huntington's disease [27], malignant melanoma [28], osteoporosis [29], and rheumatoid arthritis [30].

Because of the positive correlation between the up-regulation of QC and the development and severity of these diseases, QC is thought as a reasonable target for the discovery of disease-modifying agents [19,20,25–27,31]. Then, several compounds have been reported, which exhibited remarkable potency to prevent or treat these diseases by inhibiting QC activity [24–27,32–40]. Especially, PQ912, one QC inhibitor, has been in phase II clinical trials for AD treatment [41–43]. So, inhibition of QC by small molecule inhibitors may offer a novel approach for the disease-modifying therapies in AD and other disorders related with up-regulation of QC.

To explore new QC inhibitors, a series of diphenyl conjugated imidazole (DPCI) derivatives were designed, synthesized and evaluated as potential anti-AD chemicals in our previous report [40]. Here, anti-inflammation effects of **DPCI-23** (Fig. 1A, IC_{50} = 0.50 μM, [40]) in AD mice and LPS-induced inflammatory mice were presented furtherly. The potency of the selected compound exhibited in this research supports the employment of QC inhibitor in the treatment of these chronic diseases mediated by up-regulated QC.

2. Materials and methods

2.1. DPCI-23

DPCI-23 ($C_{19}H_{20}FN_3$, MW: 309.38) was synthesized in our lab. Stock solution (10 mg/mL) was prepared in 100 μL DMSO containing 60 mg **DPCI-23** and 50 mg Solutol HS15 (BASF, Ludwigshafen, Germany), and diluted in sterilized saline to make secondary stock solution (10 mg/mL).

2.2. Mice and treatment

Animal experiments were in line with the guidelines for the welfare of experimental animals, approved by the Animal Ethic Committee at Shenzhen University and carried out in accordance with the approved guidelines. B6C3-Tg (APPswe/PSEN1dE9)85Dbo/J double transgenic mice (5 month, female) were obtained from Guangdong Medical Laboratory Animal Center (Foshan, China) as certified AD model mice and housed in Shenzhen University Animal Care Facility in a 12 h light/dark cycle with free access to food and water. Mice (n = 8 mice/group) were treated with contrast solution (Control), 1.7 mg/kg (Low dose) and 5 mg/kg (High dose) of **DPCI-23** respectively by intraperitoneal injection for 4 weeks, 3 times per week.

For LPS-induced inflammatory model, C57BL/6 mice (6 month, female) were obtained from Beijing Vital River Laboratory Animal Technology Co., Ltd. (Beijing, China) and divided into 3 groups (n = 10 mice/group): Control, Inflammation and **DPCI-23**. Mice in **DPCI-23** and Inflammation were intraperitoneally injected with 100 μL LPS (1 mg/mL, Sigma-Aldrich, St. Louis, USA) for 3 days, then treated with **DPCI-23** (5 mg/kg) and control solution respectively for one day. Mice in Control were intraperitoneally injected with sterilized saline only.

2.3. Behavioral tests

2.3.1. Open field

Exploration was assessed by placing mice individually in the center of a 36 × 36 cm black box with 2 mm white lines drawn on the bottom, separating the space of box into 36 small squares with the width of 6 cm. The behavior of mice was recorded for 3 min. The horizontal movement (*e.g.* walk, run) was evaluated by counting the number of squares while the vertical movement (*e.g.* stand, jump) was examined according to the number of action [44].

2.3.2. Nest construction

Mice were housed individually in cages each containing eight pieces of square paper with the width of 5 cm for nesting. The nests were assessed according to a four-point scale after 24 h: 0 point, the paper remained > 90% intact; 1 point, the paper remained 60–90% intact with no identifiable nest; 2 points, the paper was 30–60% intact with an identifiable nest shape; 3 points, the paper was 10–30% intact with a noticeably identifiable nest [45].

2.3.3. T-slot water maze

T-slot water maze assay was performed according to Paban et al' method with following modifications [46]. Simply, the water maze consisted of a transparent T-slot (74 × 60 × 14 cm) filled with water (24 to 26 °C, 8 cm deep). A circular platform (5 cm in diameter) was located at one arm, and three drawings were pasted on one wall of the slot. Mice were allowed to enter the slot from 3 random directions and swim until they found the platform in 60 s. Mice were guided to the platform and allowed to rest for 10 s when they could not reach the platform in time. Mice were subjected to two trials per day with an interval of 20 min for 3 days. The spatial learning of mice was determined by the time they spent reaching the platform on the 4th day.

2.4. QC activity assay

For AD mice, one day after the behavioral testing, mice were sacrificed by CO_2 inhalation; the brains were removed, divided into 3 groups (cortex, hippocampus, hemisphere) and homogenized in chilled PBS (m/v 1:9) complemented with 1% (*v*/v) protease inhibitors (Roche, Basel, Switzerland). After centrifugation, the supernatants were used for QC activity assay according to the report [47]. Briefly, reactions were started by the addition of supernatants into the assay buffer (30 U/mL glutamate dehydrogenase, 3.84 mM Gln-Gln, 14 mM α-Ketoglutaric acid, 0.3 mM NADH, 150 mM NaCl, 50 mM Tris, pH 8.0) at 25 °C. Activity (μM/min) was monitored by recording the decrease in absorbance at 340 nm for 15 min with an interval of 30 s using Thermo Multiscan GO 1510 spectrophotometer (Thermo Fisher Scientific, Vantaa, Finland).

QC activities in the supernatants of cortex and hippocampus from LPS-induced inflammatory model mice were determined using the same

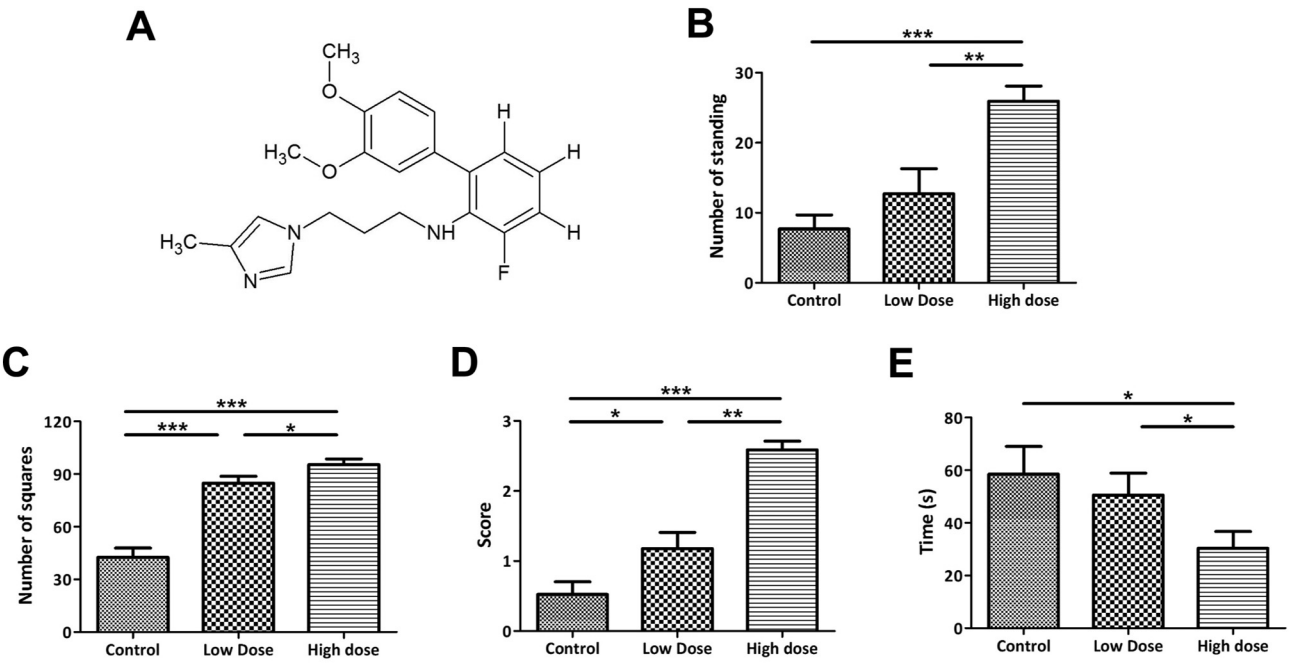

Fig. 1. Effects of DPCI-23 on cognitive and behavioral performance in AD mice.
(**A**)The structure of **DPCI-23**; (**B**,**C**) Open field. Mice were placed individually in the center of a 36 × 36 cm black box with 2 mm white lines drawn on the bottom, separating the space of box into 36 small squares with the width of 6 cm. The behavior of mice was recorded for 3 min. The horizontal movement was evaluated by counting the number of squares while the vertical movement was examined according to the number of action; (**D**) Nest construction. Mice were housed individually in cages each containing eight pieces of square paper with the width of 5 cm for nesting. The nests were assessed according to a four-point scale after 24 h; (**E**) T-slot water maze. The water maze consisted of a transparent T-slot (74 × 60 × 14 cm) filled with water (24 to 26 °C, 8 cm deep). A circular platform (5 cm in diameter) was located at one arm, and three drawings were pasted on one wall of the slot. Mice were allowed to enter the slot from 3 random directions and swim until they found the platform in 60 s. Mice were guided to the platform and allowed to rest for 10 s when they could not reach the platform in time. Mice were subjected to two trials per day with an interval of 20 min for 3 days. The spatial learning of mice was determined by the time they spent reaching the platform on the 4th day. $^{*}p < 0.05$, $^{**}p < 0.01$, $^{***}p < 0.001$, $n = 8$.

assay as mentioned above.

2.5. Histology

Deeply anesthetized mice were perfused intracardially with PBS and with 4% PFA (Beijing Solarbio Science & Technology Co., Ltd., Beijing, China) for 20 min respectively. Brains were removed, fixed in 4% PFA at 4 °C overnight and dehydrated in ascending concentrations of saccharose (10%, 20%, 30%) at 4 °C. When embedded in Optimal cutting temperature Compound (Sakura Finetek Japan Co., Ltd., Tokyo, Japan), 9 μm sections were prepared, dried at 60 °C for 24 h and stored at −80 °C.

2.5.1. Immunohistochemistry

UltraSensitive™ SP (Mouse/Rabbit) IHC Kit (Fuzhou Maixin Biotech. Co., Ltd., Fuzhou, China) was used here. Briefly, pre-treated sections were incubated with 50 μL peroxidase blocking solution (Solution A) for 10 min, followed by 50 μL goat serum (Solution B). 50 μL rabbit anti-QPCT antibody [ab201172] (1:100, Abcam, Cambridge, USA), mouse monoclonal antibody against Abeta-pE3, clone 2–48 (1:200, Synaptic Systems, Goettingen, Germany) or mouse monoclonal anti-β-amyloid antibody (Sigma-Aldrich, St. Louis, USA) were added to detect QC, pE-A$\beta_{3\text{-}42}$ and total Aβs respectively. Treated with 50 μL biotin-labeled goat anti-mouse/rabbit IgG (Solution C) for 10 min at room temperature, sections were incubated with 50 μL streptavidin-peroxidase (Solution D). Staining was performed using ABC method with DAB Plus Kit (Fuzhou Maixin Biotech. Co., Ltd.), which results in a brown precipitate. Dehydration of sections was carried out with ascending concentrations of ethanol (30%, 50%, 75%, 85%, 95%, 100%), dimethylbenzene/ethanol (1:1, *v*/v) and dimethylbenzene then. Sections were mounted with Antifade Mounting Medium (Beyotime Biotechnology, Shanghai, China).

2.5.2. Thioflavin T staining

Pre-washed with PBS, sections were incubated with 100 μL 0.1% thioflavin T in 0.1N HCl at room temperature for 30 min, and mounted with Antifade Mounting Medium after washing with 75% ethanol and PBS.

2.5.3. Immunofluorescence staining

To detect microglia and astrocytes, sections pro-treated with goat serum were incubated with rabbit anti-Iba1 antibody [EPR16589] (1:100, Abcam) and GFAP rabbit polyclonal antibody (1:100, Proteintech, Rosemont, USA) at 4 °C overnight respectively. Dylight488 goat anti-rabbit IgG [H + L] (1:200, MultiSciences, Hangzhou, China) was used as secondary antibody. After washing three times with PBS, sections were mounted with Antifade Mounting Medium.

2.5.4. Imaging

Mounted sections were observed using Nikon Y-Tv 55 microscopy (Nikon, Tokyo, Japan) equipped with epifluorescence and visualized with a CCD camera (Nikon DS-RI2). Regions of dentate gyrus, CA3 and cortex were captured on six sections/animal at 10 × or 20 × magnification. Integral optical density (IOD) of images were analyzed by Image-Pro Plus 6.0 software.

2.6. ELISA

After centrifugation, the levels of IL-1β, IL-6, and TNF-α in supernatants of blood samples from AD mice were determined using Mouse IL-1β ELISA kit (GenScript USA Inc., Piscataway, USA), 96T Mouse IL-6 ELISA kit (4A biotech Co. Ltd., Beijing, China) and 96T Mouse TNF-α

ELISA kit (4A biotech Co. Ltd., Beijing, China) respectively.

The levels of IL-1β, IL-1ra, CCL2 and TNF-α in the supernatants of brain (cortex, hippocampus, hemisphere), kidney and blood from LPS-induced inflammatory mice were quantified using Mouse IL-1β ELISA kit (GenScript USA Inc., Piscataway, USA), 96T Mouse IL-1ra/IL-1F3 ELISA kit (4A biotech Co. Ltd., Beijing, China), 96T Mouse MCP-1 ELISA kit (4A biotech Co. Ltd., Beijing, China) and 96T Mouse TNF-α ELISA kit (4A biotech Co. Ltd., Beijing, China) respectively. The levels of QC in brains were determined by AMEKO Mouse QPCT ELISA kit (Shanghai Lianshuo Biological Co., Ltd., Shanghai, China). ELISA measurements were performed according to the manuals in triplicate, repeated three times.

2.7. Statistical analysis

Statistical comparisons were evaluated using SPSS 19.0 statistics software (IBM Corporation, Armonk, NY, USA). One way analysis of variance followed by S-N-K test was performed to evaluate the differences between groups and significance was considered at $p < 0.05$. All data were graphed using GraphPad Prism 5 (GraphPad Software, Inc., La Jolla, USA) and presented as mean ± standard deviation.

3. Results

3.1. DPCI-23 exhibited anti-AD and anti-inflammation effects in AD mice

3.1.1. Treatment of DPCI-23 enhanced cognitive and behavioral performance

DPCIs were designed based on the crystal structure of QC and developed as potential anti-AD chemicals. The effects of **DPCI-23**, which exhibited inhibitory potency on QC activity *in vitro*, on cognition and behavior of AD mice were examined here firstly. As we expected, the performance of AD mice treated with **DPCI-23** to move in horizontal direction and stand in vertical direction were improved remarkably in a dose-dependent manner (Fig. 1B and C). And in nest construction test, no obvious bites were observed on nesting paper in cages housing mice in control group, with the score of nest shape averaged to 0.53 (Fig. 1D). By comparison, the average scores of nest shape constructed by AD mice treated with **DPCI-23** at low and high doses were 1.18 and 2.59 respectively, with the identifiable nests distributed in cages. Besides, it was hard for mice in control group to find the right direction and reach the destination in T-slot water maze (58.53 s) (Fig. 1E). However, the average time for treated AD mice in low and high dose groups to reach the platform were reduced (50.59 and 30.37 s respectively). Data obtained in behavioral tests suggested that the treatment of **DPCI-23** significantly enhance the performance of spatial exploration, nest building, context memory and spatial learning in AD mice.

3.1.2. Treatment of DPCI-23 inhibited QC activity and reduced pE-Aβ$_{3-x}$ and Aβ plaques dramatically

To investigate the potential actions involved in the enhancement of cognitive and behavioral performance, the activity and expression of QC in AD mice brain were determined consequently. It was found that QC activities in cortex, hippocampus and hemisphere in treated AD mice were inhibited significantly in a dose-dependent manner (Fig. 2A). The irregular expression of QC in the brains of AD mice with treatment or not illustrated that the treatment exhibited no obvious effects on the expression of QC (Fig. 2B). This observation is also in line with the phenomenon that the expression of QC in different regions in brain is different. Then, the treatment of **DPCI-23** was shown to inhibit the activity of QC in AD mice brain instead of its expression.

According to the histochemical analysis, pE-Aβ$_{3-x}$ plaques in dentate gyrus, CA3 and cortex were reduced dose-dependently after the treatment. Integrated optical density (IOD) values of pE-Aβ$_{3-x}$ plaques detected in these three regions in brains of AD mice without treatment were 1871.13, 1607.01 and 1516.70 respectively. In contrast, IOD values in the brains of AD mice treated at high dose were reduced to 139.61, 242.33 and 175.29 respectively (Fig. 2C and D). Along with the reducing of pE-Aβ$_{3-x}$ plaques, the formation of total Aβ plaques in dentate gyrus, CA3 and cortex in treated AD mice was inhibited remarkably in a dose-dependent manner (Fig. 3A and C). Similar results were obtained in ThT analysis (Fig. 3B and D). The significantly increased Aβ$_{1-40}$/pE-Aβ$_{3-x}$ ratios furtherly indicated the inhibition on the transformation of Aβ to pE-Aβ in AD mice treated with **DPCI-23** (Fig. 3E). These results demonstrated that QC inhibitor could reduce the formation of pE-Aβ$_{3-x}$ plaques and total Aβ plaques by inhibiting QC activity, and supported the hypothesis that pE-Aβ could seed the aggregation and formation of total Aβ plaques in AD progress.

3.1.3. Treatment of DPCI-23 attenuated inflammatory responses significantly

The occurrence of chronic neuro-inflammation, another clinicopathologic feature of AD induced mainly by over-activated glial cells and increased inflammatory factors, is usually accompanied by the up-regulation of QC in AD brain. Here, **DPCI-23** exhibited notable effects on inflammatory responses in AD mice in a dose-dependent manner. Activations of astrocytes and microglia cells in brains were both inhibited obviously after the treatment. Few activated astrocytes and microglia cells could be detected in dentate gyrus, CA3 and cortex in AD mice treated at high hose (Fig. 4A–D). Meanwhile, levels of inflammatory factors in the serum were reduced dose-dependently in treated AD mice, for instance, the levels of IL-6, IL-1β and TNF-α were significantly reduced to 12.55, 25.86 and 162.36 pg/mL respectively after the treatment at high dose as shown in ELISA analysis (Fig. 4E–G). So, these data suggested the potency of **DPCI-23** to attenuate neuro-inflammation reactions in AD mice by inhibiting the activation of astrocytes and microglia cells and reducing the levels of inflammatory mediators.

3.2. DPCI-23 exhibited anti-inflammation effects in inflammatory mice induced by LPS

3.2.1. DPCI-23 attenuated inflammatory responses

In view of the effects on inflammation in AD model mice, anti-inflammatory effects of **DPCI-23** were furtherly assessed in a widely used inflammatory model here. LPS, known as endotoxins existing in Gram-negative bacteria, prompts acute immune responses in animals by stimulating the secretion of pro-inflammatory cytokines, eicosanoids, NO and so on through the binding with CD14/TLR4/MD2 receptor complex in cells, especially in monocytes and macrophages [48,49]. In this study, C57BL/6 mice were intraperitoneally injected with LPS for 3 days to induce inflammation responses. As a result, the contents of TNF-α, IL-1ra and CCL2 in serum were increased to 178.8, 68.6 and 265.9 pg/mL (Fig. 5A–C), the levels of TNF-α, IL-1ra and IL-1β in kidneys were evaluated to 34.2, 47.3 and 85.0 pg/mL (Fig. 5D–F), and the contents of TNF-α, IL-1ra and CCL2 in cortex, hippocampus and hemisphere of brains were increased to 87.3, 97.7 and 72.3 pg/mL (Fig. 5G), 62.2, 55.3 and 34.0 pg/mL (Fig. 5H), 15.6, 27.5 and 17.8 pg/mL (Fig. 5I), respectively. The remarkably increased pro-/inflammatory mediators shown in ELISA indicated the obvious inflammation in C57BL/6 mice after the injection of LPS.

Interestingly, the evaluations of these mediators in inflammatory mice were repressed significantly with the treatment of **DPCI-23**. The levels of TNF-α, IL-1ra and CCL2 in serum were 53.7, 40.8 and 142.1 pg/mL (Fig. 5A–C). Similarly, the contents of TNF-α, IL-1ra and IL-1β in kidneys were reduced to 19.9, 44.6 and 59.6 pg/mL obviously (Fig. 5D–F). And in cortex, hippocampus and hemisphere of treated mice, the levels of TNF-α, IL-1ra and CCL2 were also dropped to 56.9, 63.8 and 42.0 pg/mL (Fig. 5G), 18.5, 31.7 and 10.3 pg/mL (Fig. 5H), 6.2, 2.5 and 7.4 pg/mL (Fig. 5I), respectively. These data demonstrated the significant potency of QC inhibitor to attenuate inflammatory responses in inflammatory mice.

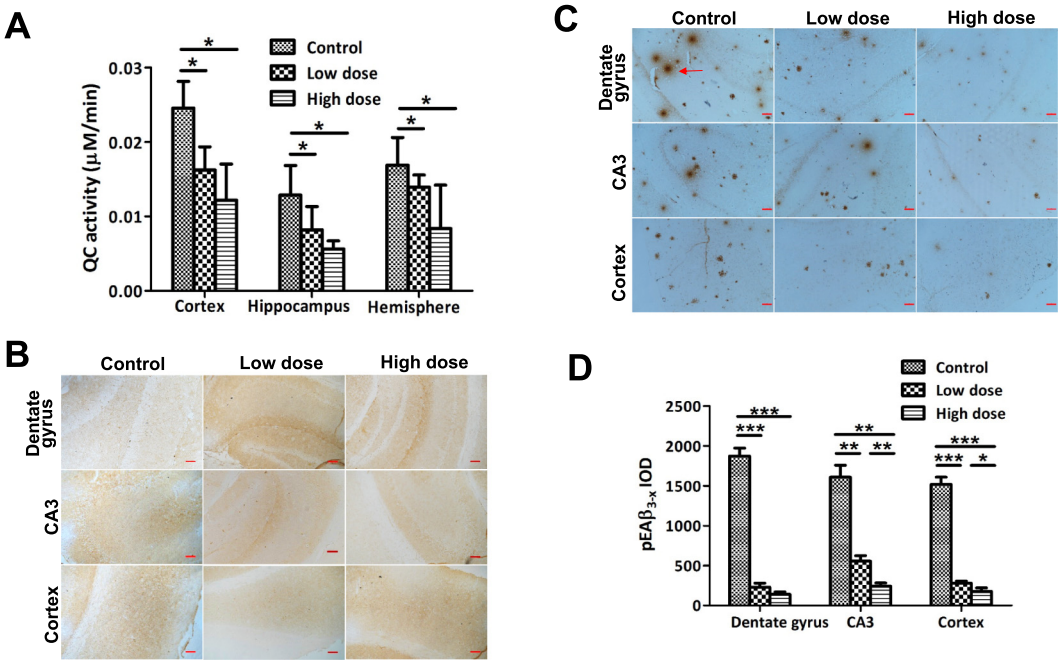

Fig. 2. Effects of DPCI-23 on QC activity and the formation of p*E*-Aβ plaques in AD mice.
(**A**) QC activity. After centrifugation, reactions were started by the addition of supernatants extracted from cortex, hippocampus and hemisphere into the assay buffer (30 U/mL glutamate dehydrogenase, 3.84 mM Gln-Gln, 14 mM α-Ketoglutaric acid, 0.3 mM NADH, 150 mM NaCl, 50 mM Tris, pH 8.0) at 25 °C. Activity (μM/min) was monitored by recording the decrease in absorbance at 340 nm for 15 min with an interval of 30 s; (**B**) The expression of QC. Pre-treated sections (9 μm) were incubated with 50 μL peroxidase blocking solution for 10 min, followed by 50 μL goat serum. 50 μL rabbit anti-QPCT antibody (1:100) was added to detect QC. Treated with 50 μL biotin-labeled goat anti-mouse/rabbit IgG for 10 min at room temperature, sections were incubated with 50 μL streptavidin-peroxidase. Staining was performed using ABC method with DAB Plus Kit; (**C**) pE-Aβ plaques. pE-$Aβ_{3-x}$ plaques were detected using mouse monoclonal antibody against Abeta-pE3, clone 2–48 (1:200). The protocol was the same as mentioned in (**B**); (**D**) IOD values of (**C**). Bar = 100 μm. $^{*}p < 0.05$, $^{**}p < 0.01$, $^{***}p < 0.001$. (**A**) $n = 5$, (**B-D**) $n = 3$.

3.2.2. DPCI-23 reduced QC activity and activation of microglia cells

The activity and expression of QC in brains of inflammatory mice treated with **DPCI-23** or not were investigated. It was shown that QC activities in cortex and hippocampus of inflammatory mice induced by the injection of LPS were increased to 0.016 and 0.028 μM/min, but the activities in cortex and hippocampus of treated mice were reduced to 0.007 and 0.003 μM/min respectively based on the data obtained in GD-QC assay (Fig. 6A). Similar as in AD mice, the treatment also exhibited no obvious effects on the irregular expression of QC in brains (Fig. 6B and C). These results suggested that up-regulated QC activity in brain of inflammatory mice induced by LPS could be inhibited by the treatment of QC inhibitor.

Analysis of the inflammatory reactions in central neuron system (CNS) was carried out to understand the anti-inflammatory potency of QC inhibitor. Over-activation of microglia and astrocytes always indicates the presence of inflammation, especially in CNS. As shown in Fig. 7A–D, over-activation of microglia and astrocytes in brain of LPS-induced inflammatory mice was observed. By contrast, over-activated microglia and astrocytes were reduced significantly after the treatment of **DPCI-23**. Results obtained here confirmed the anti-inflammation effects of QC inhibitor in widely used inflammatory model mice.

4. Discussion

Recently, QC has become an attractive target for the therapeutics of disorders such as AD, thyroid carcinomas, septic arthritis, and non-alcoholic fatty liver disease because of the positive correlation between the QC activity and the initiation of inflammation. Abnormally up-regulated QC results in the development of inflammation by catalyzing the generation of pE-modified mediators. Then, a few compounds have been designed and synthesized as QC inhibitors which exhibit notable QC inhibitory potency *in vitro* and *in vivo* [23–26,33–39]. DPCIs were reported as a series of novel QC inhibitors in our previous research [40]. To illustrate the potency of DPCIs furtherly, **DPCI-23** was selected and its effects on inflammatory reactions in AD and inflammatory model mice were assessed in this study.

Expectedly, behavioral and cognitive performance in AD mice were all improved in a dose-dependent manner after the treatment of **DPCI-23** based on behavioral tests (Fig. 1). Significantly enhanced mental state, nesting behavior, context memory and spatial learning ability of AD mice indicated the anti-AD effects of the selected compound. It was confirmed that QC activities in cortex and hippocampus in treated AD mice brains were inhibited dose-dependently (Fig. 2A). As the subsequent results, the generation of pE-Aβ and the formation of pE-Aβ plaques were inhibited remarkably (Fig. 2C and D). And the reducing of total Aβ plaques (Fig. 3), together with the increased proportion of $Aβ_{1-40}$/pE-$Aβ_{3-x}$, supported the involvement of pE-Aβ in the formation of plaques by seeding further aggregation in the presence of Aβ. These results illustrated the crucial role of up-regulated QC in the development of AD. Interestingly, the evaluation of QC activity in brains of inflammatory mice induced by the injection of LPS was observed for the first time (Fig. 6 A). The elevated QC activities were also inhibited significantly after the treatment. As similar in AD mice, this chemical exhibited no obvious effect on the expression of QC in brains of inflammatory mice (Figs. 2B, 6B and C). Although the causes up-regulating QC activity need further research, data obtained here demonstrated the inhibitory potency of **DPCI-23** on QC in both AD and inflammatory model mice.

Then, effects of **DPCI-23** on inflammatory reactions in these models were investigated. Inflammation in brains was detected firstly as QC is mainly distributed in brain [1,26,50–53]. Microglia cells are known as primary immune effector cells, and astrocytes act as supporting cells for the architecture, function and genesis of neurons [54,55]. Over-activation of microglia cells and astrocytes is thought as one of the indicators of inflammation. The robust inflammatory reactions in brain is caused mainly by “activated” microglia and astrocytes which are

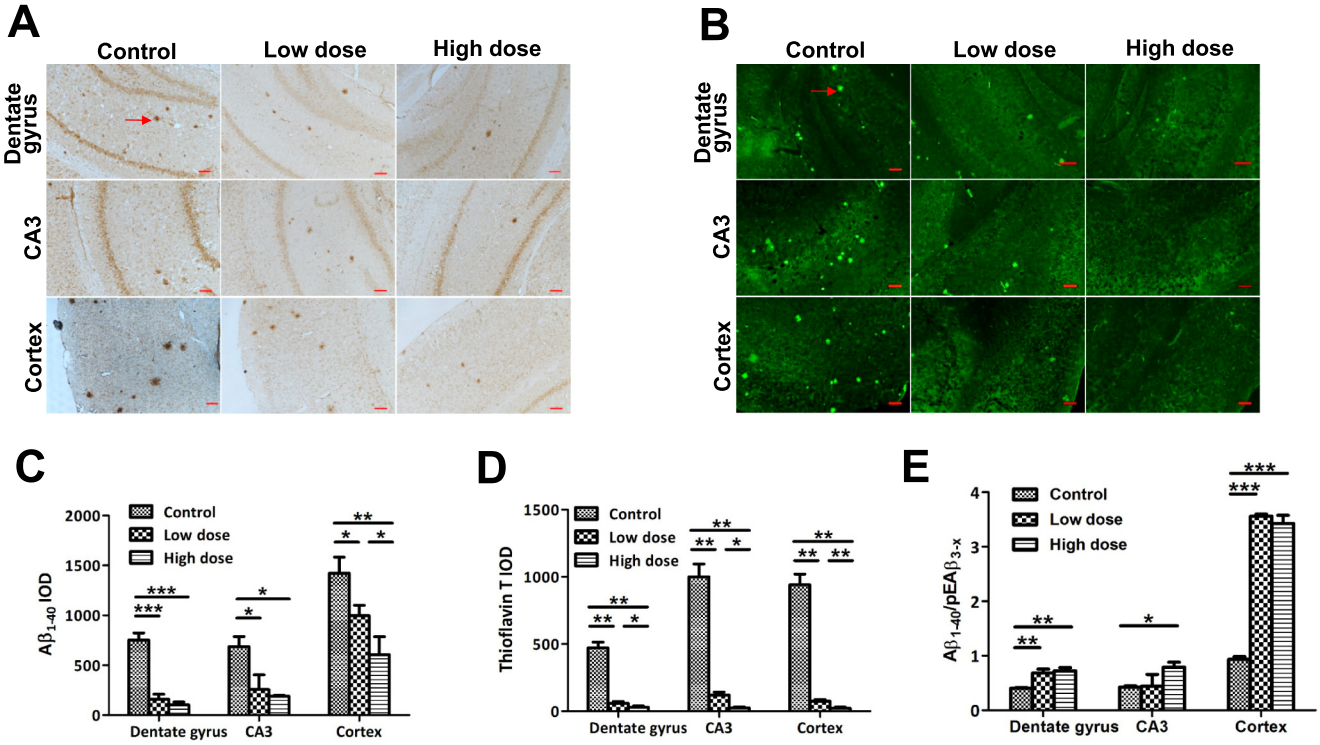

Fig. 3. Effects of DPCI-23 on the formation of Aβ plaques in AD mice.
(**A**) Aβ plaques detected by immunohistochemistry. Pre-treated sections (9 μm) were incubated with 50 μL peroxidase blocking solution for 10 min, followed by 50 μL goat serum. 50 μL mouse monoclonal anti-β-amyloid antibody was added to detect Aβ plaques. Treated with 50 μL biotin-labeled goat anti-mouse/rabbit IgG for 10 min at room temperature, sections were incubated with 50 μL streptavidin-peroxidase. Staining was performed using ABC method with DAB Plus Kit; (**B**) Aβ plaques detected by Thioflavin T staining. Pre-washed with PBS, sections were incubated with 100 μL 0.1% thioflavin T in 0.1 N HCl at room temperature for 30 min, and mounted with Antifade Mounting Medium after washing with 75% ethanol and PBS; (**C**) IOD values of (**A**); (**D**) IOD values of (**B**); (**E**) $A\beta_{1\text{-}40}$/pE-$A\beta_{3\text{-}x}$ ratios. Bar = 100 μm. $^{*}p < 0.05$, $^{**}p < 0.01$, $^{***}p < 0.001$, n = 3.

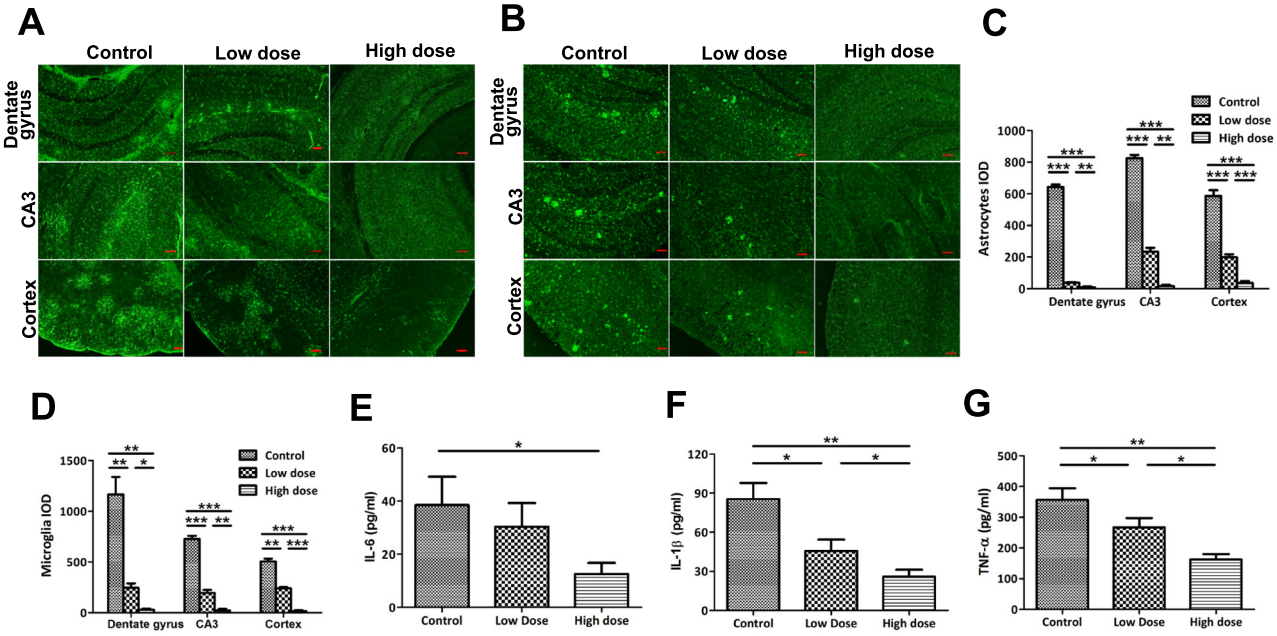

Fig. 4. Effects of DPCI-23 on inflammatory responses in AD mice.
(**A**) Astrocytes. Sections pro-treated with goat serum were incubated with GFAP rabbit polyclonal antibody (1:100) at 4 °C overnight. Dylight488 goat anti-rabbit IgG [H + L] (1:200) was used as secondary antibody. After washing three times with PBS, sections were mounted with Antifade Mounting Medium; (**B**) Microglia. Activated microglia were detected using rabbit anti-Iba1 antibody (1:100). The protocol was the same as mentioned in (**A**); (**C**, **D**) IOD values of (**A**) and (**B**) respectively; (**E**, **F**, **G**) The levels of IL-1β, IL-6, and TNF-α. The contents of these inflammation factors in serum were determined using Mouse IL-1β ELISA kit, Mouse IL-6 ELISA kit and Mouse TNF-α ELISA kit respectively. Bar = 100 μm. $^{*}p < 0.05$, $^{**}p < 0.01$, $^{***}p < 0.001$. (**A-D**) n = 3, (**E-G**) $n = 5$.

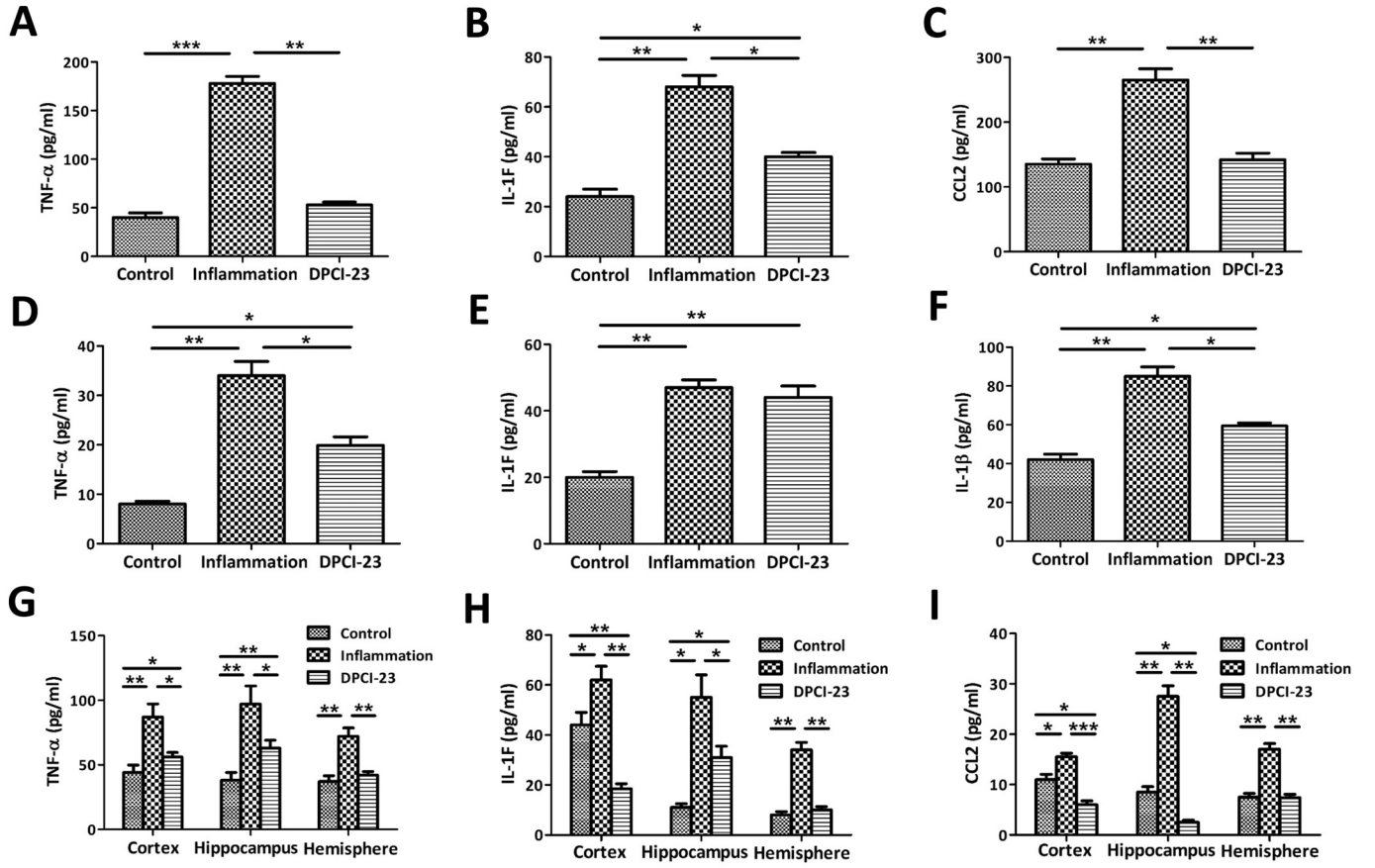

Fig. 5. Effects of DPCI-23 on inflammatory responses in LPS-induced inflammatory mice.
(**A**, **B**, **C**) The levels of TNF-α, IL-1ra and CCL2 in blood. The contents were determined using 96T Mouse TNF-α ELISA kit, 96T Mouse IL-1ra/IL-1F3 ELISA kit and 96T Mouse MCP-1 ELISA kit respectively; (**D**, **E**, **F**) The levels of TNF-α, IL-1ra and IL-1β in kidneys. The contents of IL-1β were determined using Mouse IL-1β ELISA kit; (**G**, **H**, **I**) The levels of TNF-α, IL-1ra and CCL2 in brains. $^{*}p < 0.05$, $^{**}p < 0.01$, $^{***}p < 0.001$, n = 8.

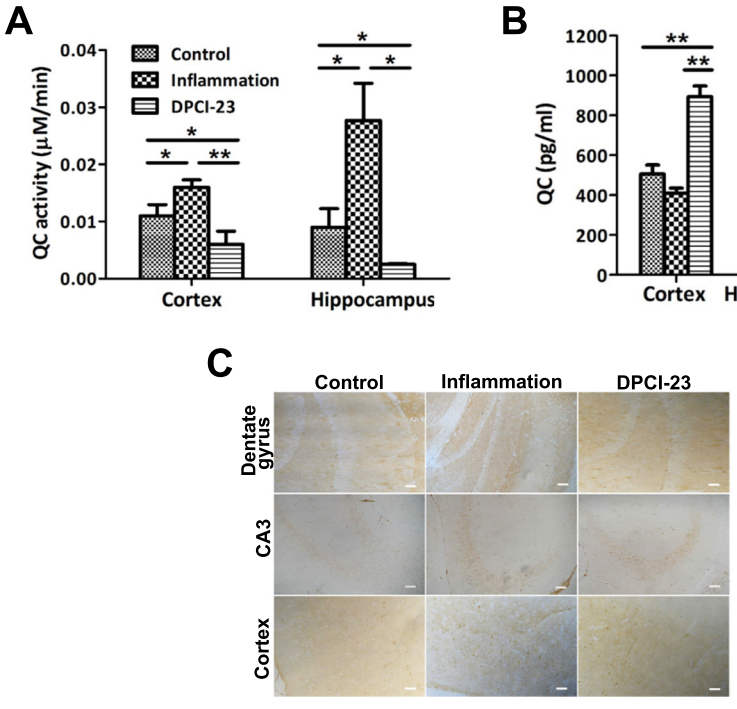

Fig. 6. Effects of DPCI-23 on QC activity in brain of LPS-induced inflammatory mice.
(**A**) QC activity. After centrifugation, reactions were started by the addition of supernatants extracted from cortex and hippocampus into the assay buffer (30 U/mL glutamate dehydrogenase, 3.84 mM Gln-Gln, 14 mM α-Ketoglutaric acid, 0.3 mM NADH, 150 mM NaCl, 50 mM Tris, pH 8.0) at 25 °C. Activity (μM/min) was monitored by recording the decrease in absorbance at 340 nm for 15 min with an interval of 30 s; (**B**) The expression of QC by ELISA. The contents of QC in cortex, hippocampus and hemisphere were determined by AMEKO Mouse QPCT ELISA kit; (**C**) The expression of QC by immunohistochemistry. Pre-treated sections (9 μm) were incubated with 50 μL peroxidase blocking solution for 10 min, followed by 50 μL goat serum. 50 μL rabbit anti-QPCT antibody (1:100) was added to detect QC. Treated with 50 μL biotin-labeled goat anti-mouse/rabbit IgG for 10 min at room temperature, sections were incubated with 50 μL streptavidin-peroxidase. Staining was performed using ABC method with DAB Plus Kit. Bar = 100 μm. $^{*}p < 0.05$, $^{**}p < 0.01$, $^{***}p < 0.001$, n = 8.

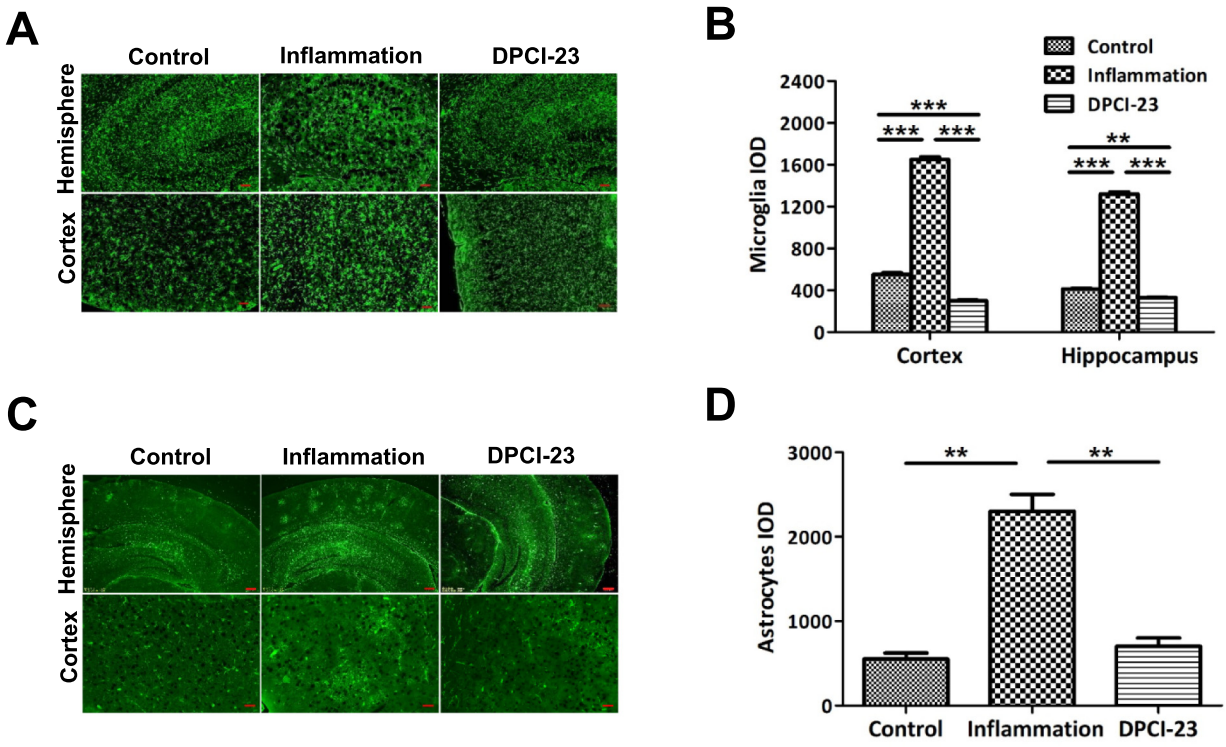

Fig. 7. Effects of DPCI-23 on inflammatory responses in brain of LPS-induced inflammatory mice.
(**A**) Microglia. Sections pro-treated with goat serum were incubated with rabbit anti-Iba1 antibody (1:100). at 4 °C overnight. Dylight488 goat anti-rabbit IgG [H + L] (1:200) was used as secondary antibody. After washing three times with PBS, sections were mounted with Antifade Mounting Medium. (**C**) Astrocytes. Activated astrocytes were detected using GFAP rabbit polyclonal antibody (1:100). The protocol was the same as mentioned in (**A**); (**B**, **D**) IOD values of (**A**) and (**C**) respectively. Bar = 200 μm. $^{*}p < 0.05$, $^{**}p < 0.01$, $^{***}p < 0.001$, n = 8.

commonly sensitive to kinds of inflammatory mediators and other abnormal factors such as pE-Aβ and Aβ plaques [56]. In AD mice, over-activated microglia cells and astrocytes in dentate gyrus, CA3 and cortex were all reduced significantly after treatment (Fig. 4). This may result from the reducing of pE-Aβ by inhibiting QC activity and the inhibition on Aβ plaques consequently after the treatment of QC inhibitor. Meanwhile, microglia cells and astrocytes in C57BL/6 mice were over-activated after the injection of LPS (Fig. 7). And the over-activation of these effector cells were inhibited notably in inflammatory mice treated with **DPCI-23**. So, it was demonstrated that QC inhibitor could attenuate inflammatory reactions in brain based on the inhibitory potency on QC activity.

Besides, increased levels of inflammatory mediators are usually considered as the bio-markers of inflammation. For instance, elevated IL-1β, IL-6 and TNF-α are used as inflammatory markers that are deleterious to neurons in AD patients [57]. It is confirmed that activation of microglia cells and astrocytes result in the generation of a large amount of cytokines and cytotoxic factors including NO, O_2^-, IL-1β, IL-6 and TNF-α [21,22]. Thus, the elevated levels of IL-1β, IL-6, and TNF-α in serum of AD mice (Fig. 4) might due to the activated microglia and astrocytes and/or other possible sources related with AD. After the treatment of **DPCI-23**, the levels of these mediators were reduced significantly in a dose-dependent manner. In C57BL/6 mice injected with LPS which prompts acute immune responses in animals by stimulating the secretion of kinds of inflammatory cytokines, levels of TNF-α, IL-1ra, IL-1β in kidneys and levels of TNF-α, IL-1ra, CCL2 in serum and brains were all increased notably (Fig. 5). But the elevation of these pro-/inflammatory factors in inflammatory mice was inhibited significantly after the treatment. These data furtherly illustrated the significant potency of QC inhibitor to attenuate inflammatory responses in AD and inflammatory mice.

5. Conclusion

Up-regulated QC could induce inflammatory reactions by catalyzing the generation of inflammatory mediators and/or activating other potential pathways. Results obtained in this research confirmed the anti-AD potency of **DPCI-23**, and more importantly, this study indicated the anti-inflammation effects of QC inhibitor in both AD and inflammatory models. Although molecular mechanisms in detail need further investigate, QC inhibitor could be used as leading agents for the treatment of these disorders. And DPCIs and corresponding research may contribute to new approaches for the prevention and treatment of inflammation-related diseases.

Declaration of Competing Interest

None.

Acknowledgement

This work was supported by the grants of National Natural Science Foundation of China (No. 81573288), Science and Technology Planning Project of Guangdong Province (No. 2013B021100022), Science and Technology Planning Project of Shenzhen City (No. JCYJ20170302144938485, JCYJ20180305163554458).

References

[1] H. Cynis, T. Hoffmann, D. Friedrich, A. Kehlen, K. Gans, M. Kleinschmidt, J.U. Rahfeld, R. Wolf, M. Wermann, A. Stephan, M. Haegele, R. Sedlmeier, S. Graubner, W. Jagla, A. Muller, R. Eichentopf, U. Heiser, F. Seifert, P.H. Quax, M.R. de Vries, I. Hesse, D. Trautwein, U. Wollert, S. Berg, E.J. Freyse, S. Schilling, H.U. Demuth, The isoenzyme of glutaminyl cyclase is an important regulator of monocyte infiltration under inflammatory conditions, EMBO Mol. Med. 3 (9) (2011) 545–558, https://doi.org/10.1002/emmm.201100158.

[2] G.N. Abraham, D.N. Podell, Pyroglutamic acid. Non-metabolic formation, function in proteins and peptides, and characteristics of the enzymes effecting its removal, Mol. Cell. Biochem. (1981) 181–190, https://doi.org/10.1007/BF00235695 38 Spec No(Pt 1).

[3] M. Hartlage-Rubsamen, K. Staffa, A. Waniek, M. Wermann, T. Hoffmann, H. Cynis, S. Schilling, H.U. Demuth, S. Rossner, Developmental expression and subcellular localization of glutaminyl cyclase in mouse brain, Int. J. Dev. Neurosci. 27 (8) (2009) 825–835, https://doi.org/10.1016/j.ijdevneu.2009.08.007.

[4] J.M. Nussbaum, S. Schilling, H. Cynis, A. Silva, E. Swanson, T. Wangsanut, K. Tayler, B. Wiltgen, A. Hatami, R. Ronicke, K. Reymann, B. Hutter-Paier, A. Alexandru, W. Jagla, S. Graubner, C.G. Glabe, H.U. Demuth, G.S. Bloom, Prion-like behaviour and tau-dependent cytotoxicity of pyroglutamylated amyloid-beta, Nature 485 (7400) (2012) 651–655, https://doi.org/10.1038/nature11060.

[5] R. Vassar, beta-Secretase, APP and Abeta in Alzheimer's disease, Subcell. Biochem. 38 (2005) 79–103 (PMID:15709474).

[6] T.A. Bayer, O. Wirths, Focusing the amyloid cascade hypothesis on N-truncated Abeta peptides as drug targets against Alzheimer's disease, Acta Neuropathol. 127 (6) (2014) 787–801, https://doi.org/10.1007/s00401-014-1287-x.

[7] T.C. Saido, T. Iwatsubo, D.M. Mann, H. Shimada, Y. Ihara, S. Kawashima, Dominant and differential deposition of distinct beta-amyloid peptide species, A beta N3(pE), in senile plaques, Neuron 14 (2) (1995) 457–466, https://doi.org/10.1016/0896-6273(95)90301-1.

[8] Y.M. Kuo, M.R. Emmerling, A.S. Woods, R.J. Cotter, A.E. Roher, Isolation, chemical characterization, and quantitation of A beta 3-pyroglutamyl peptide from neuritic plaques and vascular amyloid deposits, Biochem. Biophys. Res. Commun. 237 (1) (1997) 188–191, https://doi.org/10.1006/bbrc.1997.7083.

[9] C. D'Arrigo, M. Tabaton, A. Perico, N-terminal truncated pyroglutamyl beta amyloid peptide Abetapy3-42 shows a faster aggregation kinetics than the full-length Abeta1-42, Biopolymers 91 (10) (2009) 861–873, https://doi.org/10.1002/bip.21271.

[10] S. Jawhar, O. Wirths, T.A. Bayer, Pyroglutamate amyloid-beta (Abeta): a hatchet man in Alzheimer disease, J. Biol. Chem. 286 (45) (2011) 38825–38832, https://doi.org/10.1074/jbc.R111.288308.

[11] S. Schilling, T. Lauber, M. Schaupp, S. Manhart, E. Scheel, G. Bohm, H.U. Demuth, On the seeding and oligomerization of pGlu-amyloid peptides (in vitro), Biochemistry 45 (41) (2006) 12393–12399, https://doi.org/10.1021/bi0612667.

[12] A. Becker, S. Kohlmann, A. Alexandru, W. Jagla, F. Canneva, C. Bauscher, H. Cynis, R. Sedlmeier, S. Graubner, S. Schilling, H.U. Demuth, S. von Horsten, Glutaminyl cyclase-mediated toxicity of pyroglutamate-beta amyloid induces striatal neurodegeneration, BMC Neurosci. 14 (2013) 108, https://doi.org/10.1186/1471-2202-14-108.

[13] S. Schilling, T. Appl, T. Hoffmann, H. Cynis, K. Schulz, W. Jagla, D. Friedrich, M. Wermann, M. Buchholz, U. Heiser, S. von Horsten, H.U. Demuth, Inhibition of glutaminyl cyclase prevents pGlu-Abeta formation after intracortical/hippocampal microinjection in vivo/in situ, J. Neurochem. 106 (3) (2008) 1225–1236, https://doi.org/10.1111/j.1471-4159.2008.05471.x.

[14] A. Piccini, C. Russo, A. Gliozzi, A. Relini, A. Vitali, R. Borghi, L. Giliberto, A. Armirotti, C. D'Arrigo, A. Bachi, A. Cattaneo, C. Canale, S. Torrassa, T.C. Saido, W. Markesbery, P. Gambetti, M. Tabaton, Beta-amyloid is different in normal aging and in Alzheimer disease, J. Biol. Chem. 280 (40) (2005) 34186–34192, https://doi.org/10.1074/jbc.M501694200.

[15] L. Miravalle, M. Calero, M. Takao, A.E. Roher, B. Ghetti, R. Vidal, Amino-terminally truncated A beta peptide species are the main component of cotton wool plaques, Biochemistry 44 (32) (2005) 10810–10821, https://doi.org/10.1021/bi0508237.

[16] M. Buchholz, U. Heiser, S. Schilling, A.J. Niestroj, K. Zunkel, H.U. Demuth, The first potent inhibitors for human glutaminyl cyclase: synthesis and structure-activity relationship, J. Med. Chem. 49 (2) (2006) 664–677, https://doi.org/10.1021/jm050756e.

[17] M. Morawski, S. Schilling, M. Kreuzberger, A. Waniek, C. Jager, B. Koch, H. Cynis, A. Kehlen, T. Arendt, M. Hartlage-Rubsamen, H.U. Demuth, S. Rossner, Glutaminyl cyclase in human cortex: correlation with (pGlu)-amyloid-beta load and cognitive decline in Alzheimer's disease, J. Alzheimers Dis. 39 (2) (2014) 385–400, https://doi.org/10.3233/JAD-131535.

[18] P.A. Sykes, S.J. Watson, J.S. Temple, R.C. Bateman Jr., Evidence for tissue-specific forms of glutaminyl cyclase, FEBS Lett. 455 (1–2) (1999) 159–161, https://doi.org/10.1016/S0014-5793(99)00872-8.

[19] M.T. Valenti, S. Bolognin, C. Zanatta, L. Donatelli, G. Innamorati, M. Pampanin, G. Zanusso, P. Zatta, L.D. Carbonare, Increased glutaminyl cyclase expression in peripheral blood of Alzheimer's disease patients, J. Alzheimers Dis. 34 (1) (2013) 263–271, https://doi.org/10.3233/JAD-120517.

[20] S. Schilling, T. Hoffmann, S. Manhart, M. Hoffmann, H.U. Demuth, Glutaminyl cyclases unfold glutamyl cyclase activity under mild acid conditions, FEBS Lett. 563 (1–3) (2004) 191–196, https://doi.org/10.1016/S0014-5793(04)00300-X.

[21] S. Mandrekar-Colucci, G.E. Landreth, Microglia and inflammation in Alzheimer's disease, CNS Neurol. Disord. Drug Targets 9 (2) (2010) 156–167, https://doi.org/10.2174/187152710791012071.

[22] A. Salminen, J. Ojala, A. Kauppinen, K. Kaarniranta, T. Suuronen, Inflammation in Alzheimer's disease: amyloid-beta oligomers trigger innate immunity defence via pattern recognition receptors, Prog. Neurobiol. 87 (3) (2009) 181–194, https://doi.org/10.1016/j.pneurobio.2009.01.001.

[23] K. Westin, P. Buchhave, H. Nielsen, L. Minthon, S. Janciauskiene, O. Hansson, CCL2 is associated with a faster rate of cognitive decline during early stages of Alzheimer's disease, PLoS One 7 (1) (2012) e30525, , https://doi.org/10.1371/journal.pone.0030525.

[24] A. Kehlen, M. Haegele, K. Menge, K. Gans, U.D. Immel, C. Hoang-Vu, T. Klonisch, H.U. Demuth, Role of glutaminyl cyclases in thyroid carcinomas, Endocr. Relat. Cancer 20 (1) (2013) 79–90, https://doi.org/10.1530/ERC-12-0053.

[25] A. Hellvard, K. Maresz, S. Schilling, S. Graubner, U. Heiser, R. Jonsson, H. Cynis, H.U. Demuth, J. Potempa, P. Mydel, Glutaminyl cyclases as novel targets for the treatment of septic arthritis, J. Infect. Dis. 207 (5) (2013) 768–777, https://doi.org/10.1093/infdis/jis729.

[26] H. Cynis, A. Kehlen, M. Haegele, T. Hoffmann, U. Heiser, M. Fujii, Y. Shibazaki, H. Yoneyama, S. Schilling, H.U. Demuth, Inhibition of glutaminyl cyclases alleviates CCL2-mediated inflammation of non-alcoholic fatty liver disease in mice, Int. J. Exp. Pathol. 94 (3) (2013) 217–225, https://doi.org/10.1111/iep.12020.

[27] M. Jimenez-Sanchez, W. Lam, M. Hannus, B. Sonnichsen, S. Imarisio, A. Fleming, A. Tarditi, F. Menzies, T.E. Dami, C. Xu, E. Gonzalez-Couto, G. Lazzeroni, F. Heitz, D. Diamanti, L. Massai, V.P. Satagopam, G. Marconi, C. Caramelli, A. Nencini, M. Andreini, G.L. Sardone, N.P. Caradonna, V. Porcari, C. Scali, R. Schneider, G. Pollio, C.J. O'Kane, A. Caricasole, D.C. Rubinsztein, siRNA screen identifies QPCT as a druggable target for Huntington's disease, Nat. Chem. Biol. 11 (5) (2015) 347–354, https://doi.org/10.1038/nchembio.1790.

[28] V. Muthusamy, S. Duraisamy, C.M. Bradbury, C. Hobbs, D.P. Curley, B. Nelson, M. Bosenberg, Epigenetic silencing of novel tumor suppressors in malignant melanoma, Cancer Res. 66 (23) (2006) 11187–11193, https://doi.org/10.1158/0008-5472.CAN-06-1274.

[29] Y. Ezura, M. Kajita, R. Ishida, S. Yoshida, H. Yoshida, T. Suzuki, T. Hosoi, S. Inoue, M. Shiraki, H. Orimo, M. Emi, Association of multiple nucleotide variations in the pituitary glutaminyl cyclase gene (QPCT) with low radial BMD in adult women, J. Bone Miner. Res. Off. J. Am. Soc. Bone Miner. Res. 19 (8) (2004) 1296–1301, https://doi.org/10.1359/JBMR.040324.

[30] F.M. Batliwalla, E.C. Baechler, X. Xiao, W. Li, S. Balasubramanian, H. Khalili, A. Damle, W.A. Ortmann, A. Perrone, A.B. Kantor, P.S. Gulko, M. Kern, R. Furie, T.W. Behrens, P.K. Gregersen, Peripheral blood gene expression profiling in rheumatoid arthritis, Genes Immun. 6 (5) (2005) 388–397, https://doi.org/10.1038/sj.gene.6364209.

[31] J.A. Ratnayaka, L.C. Serpell, A.J. Lotery, Dementia of the eye: the role of amyloid beta in retinal degeneration, Eye 29 (8) (2015) 1013–1026, https://doi.org/10.1038/eye.2015.100.

[32] S. Schilling, A.J. Niestroj, J.U. Rahfeld, T. Hoffmann, M. Wermann, K. Zunkel, C. Wasternack, H.U. Demuth, Identification of human glutaminyl cyclase as a metalloenzyme. Potent inhibition by imidazole derivatives and heterocyclic chelators, J. Biol. Chem. 278 (50) (2003) 49773–49779, https://doi.org/10.1074/jbc.M309077200.

[33] M. Buchholz, A. Hamann, S. Aust, W. Brandt, L. Bohme, T. Hoffmann, S. Schilling, H.U. Demuth, U. Heiser, Inhibitors for human glutaminyl cyclase by structure based design and bioisosteric replacement, J. Med. Chem. 52 (22) (2009) 7069–7080, https://doi.org/10.1021/jm900969p.

[34] P.T. Tran, V.H. Hoang, S.A. Thorat, S.E. Kim, J. Ann, Y.J. Chang, D.W. Nam, H. Song, I. Mook-Jung, J. Lee, J. Lee, Structure-activity relationship of human glutaminyl cyclase inhibitors having an N-(5-methyl-1H-imidazol-1-yl)propyl thiourea template, Bioorg. Med. Chem. 21 (13) (2013) 3821–3830, https://doi.org/10.1016/j.bmc.2013.04.005.

[35] D. Ramsbeck, M. Buchholz, B. Koch, L. Bohme, T. Hoffmann, H.U. Demuth, U. Heiser, Structure-activity relationships of benzimidazole-based glutaminyl cyclase inhibitors featuring a heteroaryl scaffold, J. Med. Chem. 56 (17) (2013) 6613–6625, https://doi.org/10.1021/jm4001709.

[36] S. Hielscher-Michael, C. Griehl, M. Buchholz, H.U. Demuth, N. Arnold, L.A. Wessjohann, Natural products from microalgae with potential against Alzheimer's disease: sulfolipids are potent glutaminyl cyclase inhibitors, Mar. Drugs 14 (11) (2016), https://doi.org/10.3390/md14110203.

[37] V.H. Hoang, P.T. Tran, M. Cui, V.T. Ngo, J. Ann, J. Park, J. Lee, K. Choi, H. Cho, H. Kim, H.J. Ha, H.S. Hong, S. Choi, Y.H. Kim, J. Lee, Discovery of potent human glutaminyl cyclase inhibitors as anti-Alzheimer's agents based on rational design, J. Med. Chem. 60 (6) (2017) 2573–2590, https://doi.org/10.1021/acs.jmedchem.7b00098.

[38] M. Szaszko, I. Hajdu, B. Flachner, K. Dobi, C. Magyar, I. Simon, Z. Lorincz, Z. Kapui, T. Pazmany, S. Cseh, G. Dorman, Identification of potential glutaminyl cyclase inhibitors from lead-like libraries by in silico and in vitro fragment-based screening, Mol. Divers. 21 (1) (2017) 175–186, https://doi.org/10.1007/s11030-016-9717-4.

[39] V.T.H. Ngo, V.H. Hoang, P.T. Tran, J. Ann, M. Cui, G. Park, S. Choi, J. Lee, H. Kim, H.J. Ha, K. Choi, Y.H. Kim, J. Lee, Potent human glutaminyl cyclase inhibitors as potential anti-Alzheimer's agents: structure-activity relationship study of Arg-mimetic region, Bioorg. Med. Chem. 26 (5) (2018) 1035–1049, https://doi.org/10.1016/j.bmc.2018.01.015.

[40] M. Li, Y. Dong, X. Yu, Y. Li, Y. Zou, Y. Zheng, Z. He, Z. Liu, J. Quan, X. Bu, H. Wu, Synthesis and evaluation of diphenyl conjugated imidazole derivatives as potential glutaminyl cyclase inhibitors for treatment of Alzheimer's disease, J. Med. Chem. 60 (15) (2017) 6664–6677, https://doi.org/10.1021/acs.jmedchem.7b00648.

[41] T. Hoffmann, A. Meyer, U. Heiser, S. Kurat, L. Bohme, M. Kleinschmidt, K.U. Buhring, B. Hutter-Paier, M. Farcher, H.U. Demuth, I. Lues, S. Schilling, Glutaminyl cyclase inhibitor PQ912 improves cognition in mouse models of Alzheimer's disease-studies on relation to effective target occupancy, J. Pharmacol. Exp. Ther. 362 (1) (2017) 119–130, https://doi.org/10.1124/jpet.117.240614.

[42] I. Lues, F. Weber, A. Meyer, U. Buhring, T. Hoffmann, K. Kuhn-Wache, S. Manhart, U. Heiser, R. Pokorny, J. Chiesa, K. Glund, A phase 1 study to evaluate the safety and pharmacokinetics of PQ912, a glutaminyl cyclase inhibitor, in healthy subjects, Alzheimers Dement. 1 (3) (2015) 182–195, https://doi.org/10.1016/j.trci.2015.08.002.

[43] P. Scheltens, M. Hallikainen, T. Grimmer, T. Duning, A.A. Gouw, C.E. Teunissen, A.M. Wink, P. Maruff, J. Harrison, C.M. van Baal, S. Bruins, I. Lues, N.D. Prins, Safety, tolerability and efficacy of the glutaminyl cyclase inhibitor PQ912 in

Alzheimer's disease: results of a randomized, double-blind, placebo-controlled phase 2a study, Alzheimers Res. Ther. 10 (1) (2018) 107, https://doi.org/10.1186/s13195-018-0431-6.
[44] R.M. Deacon, L.L. Cholerton, K. Talbot, R.G. Nair-Roberts, D.J. Sanderson, C. Romberg, E. Koros, K.D. Bornemann, J.N. Rawlins, Age-dependent and -independent behavioral deficits in Tg2576 mice, Behav. Brain Res. 189 (1) (2008) 126–138, https://doi.org/10.1016/j.bbr.2007.12.024.
[45] R.M. Deacon, Assessing nest building in mice, Nat. Protoc. 1 (3) (2006) 1117–1119, https://doi.org/10.1038/nprot.2006.170.
[46] V. Paban, C. Manrique, M. Filali, S. Maunoir-Regimbal, F. Fauvelle, B. Alescio-Lautier, Therapeutic and preventive effects of methylene blue on Alzheimer's disease pathology in a transgenic mouse model, Neuropharmacology 76 (Pt A) (2014) 68–79, https://doi.org/10.1016/j.neuropharm.2013.06.033.
[47] S. Schilling, T. Hoffmann, M. Wermann, U. Heiser, C. Wasternack, H.U. Demuth, Continuous spectrometric assays for glutaminyl cyclase activity, Anal. Biochem. 303 (1) (2002) 49–56, https://doi.org/10.1006/abio.2001.5560.
[48] E.T. Rietschel, T. Kirikae, F.U. Schade, U. Mamat, G. Schmidt, H. Loppnow, A.J. Ulmer, U. Zahringer, U. Seydel, F. Di Padova, et al., Bacterial endotoxin: molecular relationships of structure to activity and function, FASEB J. 8 (2) (1994) 217–225, https://doi.org/10.1096/fasebj.8.2.8119492.
[49] A.K. Abbas, A.H. Lichtman, Basic Immunology: Functions and Disorders of the Immune System, 2nd ed., Elsevier Saunders, Philadelphia, PA, 2006.
[50] A. Kehlen, M. Haegele, L. Bohme, H. Cynis, T. Hoffmann, H.U. Demuth, N-terminal pyroglutamate formation in CX3CL1 is essential for its full biologic activity, Biosci. Rep. 37 (4) (2017), https://doi.org/10.1042/BSR20170712.
[51] M. Hartlage-Rubsamen, A. Waniek, J. Meissner, M. Morawski, S. Schilling, C. Jager, M. Kleinschmidt, H. Cynis, A. Kehlen, T. Arendt, H.U. Demuth, S. Rossner, Isoglutaminyl cyclase contributes to CCL2-driven neuroinflammation in Alzheimer's disease, Acta Neuropathol. 129 (4) (2015) 565–583, https://doi.org/10.1007/s00401-015-1395-2.
[52] Y.L. Chen, K.F. Huang, W.C. Kuo, Y.C. Lo, Y.M. Lee, A.H. Wang, Inhibition of glutaminyl cyclase attenuates cell migration modulated by monocyte chemoattractant proteins, Biochem. J. 442 (2) (2012) 403–412, https://doi.org/10.1042/BJ20110535.
[53] M.F. Ling, A.D. Luster, Novel approach to inhibiting chemokine function, EMBO Mol. Med. 3 (9) (2011) 510–512, https://doi.org/10.1002/emmm.201100161.
[54] S. Fuller, M. Steele, G. Munch, Activated astroglia during chronic inflammation in Alzheimer's disease–do they neglect their neurosupportive roles? Mutat. Res. 690 (1–2) (2010) 40–49, https://doi.org/10.1016/j.mrfmmm.2009.08.016.
[55] I. Blasko, M. Stampfer-Kountchev, P. Robatscher, R. Veerhuis, P. Eikelenboom, B. Grubeck-Loebenstein, How chronic inflammation can affect the brain and support the development of Alzheimer's disease in old age: the role of microglia and astrocytes, Aging Cell 3 (4) (2004) 169–176, https://doi.org/10.1111/j.1474-9728.2004.00101.x.
[56] S.W. Barger, Astrocytes and microgliain Alzheimer's disease, Adv. Mol. Cell Biol. 31 (2003) 883–899, https://doi.org/10.1016/S1569-2558(03)31039-2.
[57] E. Bagyinszky, V.V. Giau, K. Shim, K. Suk, S.S.A. An, S. Kim, Role of inflammatory molecules in the Alzheimer's disease progression and diagnosis, J. Neurol. Sci. 376 (2017) 242–254, https://doi.org/10.1016/j.jns.2017.03.031.